

1. Supernovae of Type II

SNII result from core collapse in massive stars once the core has burned Si into Fe and there is no more energy to be gained by further nuclear fusion reactions. The mass range of the progenitor stars is wide, from perhaps 8 to $100 M_{\odot}$, and hence the characteristics of the resulting SN, including the luminosity at maximum light, can vary a lot. This makes SNII much less useful as cosmological probes than other types of SN.

1.1. Maximum Density

The maximum possible density for normal matter is that of the nucleons within an atomic nucleus, assumed to prevail over the entire volume of the gas. We assume the material is pure ^{56}Fe , and the radius of an atomic nucleus of ^{56}Fe is 3 fermis (1 fermi = 10^{-13} cm).

Then $\rho_{max} \equiv \rho_{nuc}$, where

$$\rho_{nuc} \approx \frac{56(1.6 \times 10^{-24})}{(4/3)\pi r_{nuc}^3} \approx 8 \times 10^{14} \text{ gm/cm}^3 \approx 10^{15} \text{ gm/cm}^3$$

At that high ρ , one has fully packed nuclear material. The equation of state then becomes very stiff, and it is difficult to achieve a still higher ρ .

1.2. Massive Star Evolution (Pre-SN)

The table below, taken from the work of Arnett and collaborators (1989, ARAA, 27, 641), shows that although core H burning in a $20M_{\odot}$ star may last 10^7 yr and core He burning may last 10^6 yr, events move very rapidly as nuclear burning involves heavier fuels. Si burning in the core of such a star takes only 2 days ! This is because the binding energy difference per nucleon B/A for heavy nuclei does not increase much as A increases, so the

amount of energy liberated in a typical nuclear fusion reaction is low, while the luminosity of a high mass star is very large.

Si burning produces Fe. It requires $\rho \sim 5 \times 10^7$ gm/cm³, $T \sim 4 \times 10^9$ K, and generates in the core of a $20M_{\odot}$ star a photon luminosity of 4×10^{38} ergs and a neutrino luminosity of 3×10^{45} ergs; note the very high ν luminosities for the latter stages of burning in the table, $L(\text{phot}) < L(\nu)$ at all subsequent stages after He burning, and very high L_{ν} , which increases rapidly in the later stages prior to core collapse, unlike $L(\text{phot})$.

When Si burning is occurring, the core of the star is effectively a degenerate white dwarf, with composition mostly Si mixed with some Fe, which is the product of burning Si. The core has a mass of $\sim 1.2M_{\odot}$ (close to the Chandrasekhar mass limit for a stable white dwarf with that chemical composition).

In the normal course of stellar evolution, as fuel in the core of the star is exhausted, the core undergoes gravitational contraction, it heats up (virial theorem), a new fuel ignites, raising both T and P , contraction stops, and the core expands back out.

For a Fe core, no more energy from nuclear fusion is available, the core contracts gravitationally, and nominally T should increase from this, but the energy loss via neutrinos is very high, the gas is highly degenerate, and there is no new nuclear source. So this leads to further contraction, to a decrease in the mean kinetic energy/nucleon, a decrease in pressure, and finally to collapse when the core becomes dynamically unstable or $M(\text{core}) > M(\text{Chandrasekhar})$ for the appropriate chemical composition (mostly Fe).

1.3. Core Collapse in Massive Stars

The timescale for the collapse phase is very short. Recall that the dynamical timescale t_{dyn} for the Sun is about 1 hour, and $t_{dyn} \sim 1/\sqrt{G\rho}$. For $\rho \sim 10^9$ gm/cm³, $t_{dyn} < 1$ sec. The

Table 1. Burning Stages in the Evolution of a $20M_{\odot}$ Star

Fuel	ρ_c (gm/cm^3)	T_c (10^9 K)	τ (yr)	$L(\text{phot})$ (erg/sec)	$L(\nu)$ (erg/sec)
H	5.6 (0)	0.040	1.0(7)	2.7(38)	...
He	9.4(2)	0.19	9.5(5)	5.3(38)	< 1.0(36)
C	2.7(5)	0.81	3.0(2)	4.3(38)	7.4(39)
Ne	4.0(6)	1.7	3.8(−1)	4.4(38)	1.2(43)
O	6.0(6)	2.1	5.0(−1)	4.4(38)	7.4(43)
Si	4.9(7)	3.7	2 days	4.4(38)	3.1(45)

$A(B)$ denotes $A \times 10^B$.

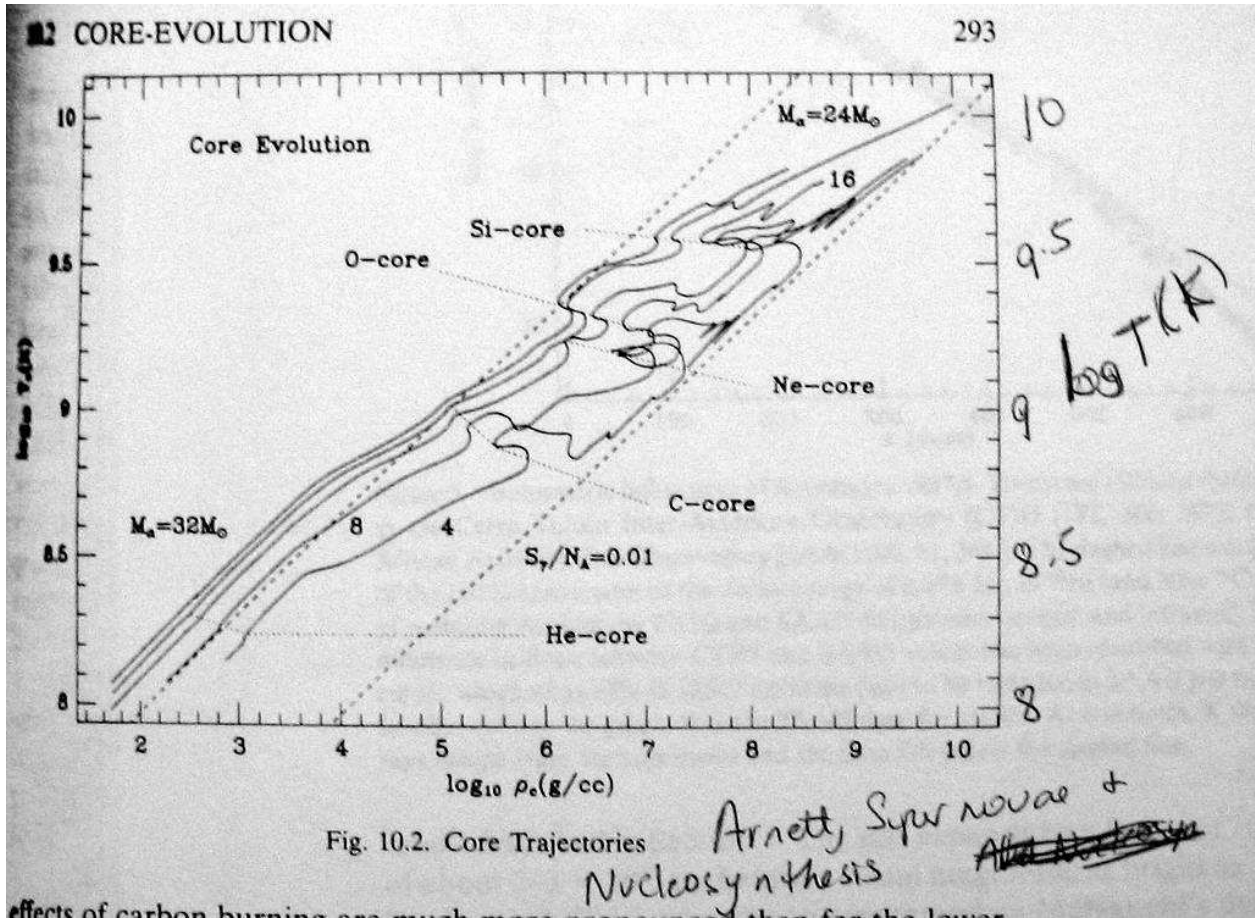


Fig. 1.— The evolutionary path of a star with 4 to 32 M_\odot in the $\rho - T$ plane. The various phases of burning are marked, from He to Si. The axes both have log scales. This figure is from Dave Arnett's book "Supernovae and Nucleosynthesis".

collapse is VERY fast.

The maximum mass of a neutron star is derived from relativistic degeneracy in the same way as is done for white dwarfs. The result for both is $M_{max}/M_{\odot} = 1.46(2/\mu_e)^2$. For a white dwarf, $\mu_e = 2$ but for a neutron star, $\mu_e = 1$, so $M_{max} = 5.8M_{\odot}$. If the mass of the core of the star at the time when Si burning is completed and the core is mostly Fe exceeds that value, collapse will lead to the formation of a black hole, otherwise a neutron star will be formed.

Assume we have a $8M_{\odot}$ star at the time of Si burning (the initial mass may have been substantially larger, mass loss is important at late stages), with a $1.2 M_{\odot}$ core consisting of pure Fe. Collapse produces a neutron star. The core mass is unchanged. We calculate the radius of the neutron star using the mass – radius relationship for non-relativistic degenerate objects, replacing m_e by m_n and setting μ_e to 2, as $\mu_e \approx 2/(1 + X)$, but there is no hydrogen left. So in the non-relativistic limit, $M/M_{\odot} \sim 10^{-6}(R/R_{\odot})(2/\mu_e)^5$ for a degenerate electron gas (i.e. white dwarfs), and $M/M_{\odot} \sim 5 \times 10^{-15}(R/R_{\odot})$ for neutron stars. Thus ρ increases from $\sim 10^9$ gm/cm³ to $\rho \sim 10^{15}$ gm/cm³, which is the same as what we calculated approximately above for ρ_{max} , the maximum possible density for nucleons.

We now estimate the difference in gravitational potential energy between an extremely compact tightly bound neutron star and a white dwarf (also compact, but not as extreme). Recall that $\Omega = -qGM^2/R = -3.8 \times 10^{38}$ ergs for the Sun. For the stellar core, $\Delta\Omega \approx GM_c^2/R(ns)$, since $R(ns) \ll R(WD)$. $\Delta\Omega \sim 6 \times 10^{53}$ ergs. This is the energy of the core collapse which is available to power the SN.

Due to the extremely high density, there are a number of phenomena which occur during core collapse that do not occur in normal stellar interiors. These include: electron capture by nuclei ($p + e^- \rightarrow n + \nu_e$), neutronization, extremely large energy losses from neutrinos, pair production, photodisintegration and inverse β -decays. We discuss these in turn below.

1.4. Photodisintegration

At $T \gtrsim 10^9$ K, photons become very energetic. They are capable of “splitting” an atomic nucleus when they impact one. We thus could have a reaction $\gamma + {}^{56}\text{Fe} \rightleftharpoons 13 {}^4\text{He} + 4n$. The energy required for this is $Q = [13m({}^4\text{He}) + 4m_n - m({}^{56}\text{Fe})]c^2 \approx 124$ MeV.

Recall that $T \sim 1.2 \times 10^4$ K corresponds to an energy of 1 eV, so for $kT = 124$ MeV, we require $T \approx 1.5 \times 10^{12}$ K, an extremely high T reached only in SN (and the Big Bang).

We can calculate the fraction of the Fe nuclei that are photodissociated.

$$\frac{n_\alpha^{13} n_n^4}{n_{56}} = \frac{g_4^{13} g_n^4}{g_{56}} \left(\frac{C_4^{13} C_n^4}{C_{56}} \right) e^{-124.4 \text{ MeV}/kT}$$

where C for each reactant is $[2\pi mkT/h^2]^{3/2}$ and the statistical weights are $g_n = 2$ (2 spin states for neutrons) and $g_4 = g_{56} = 1$ (both in spin 0 ground states).

When $\rho \sim 10^9$ gm/cm³ and $T \sim 10^{10}$ K, the above equation shows that 3/4 of the nuclei of ${}^{56}\text{Fe}$ have been photodisintegrated. This is a prelude to full neutronization where with further electron captures the α particles break up into individual neutrons.

1.5. Neutronization

Neutrons have a higher mass than protons, where $[m(n) - m(p)]c^2 = 1.3$ MeV. Normally neutrons decay into protons on the relatively short timescale of ~ 900 sec via the reaction $n \rightarrow p + e^- + \nu_e$.

However, neutrons cannot decay if all the Fermi states allowed for the electron are already filled up to its maximum energy of 1.3 MeV, where $E(\text{tot}) = m_e c^2 + E_F = m_e c^2 + 1.3$ MeV. So if $E_F \gtrsim 1.3$ MeV for electrons, the neutron cannot decay. We calculate the required

density, recalling:

$$p_F = h \left[\frac{3n_e}{8\pi} \right]^{1/3} \quad n_e = \frac{(8/3)\pi p_F^3}{h^3} \quad (p_F c)^2 = E(\text{tot})^2 - (m_e^2 c^2)^2$$

where the extra factor of 2 in the equation for n_e is for the two spin states and E_F is the Fermi energy.

If $\rho > \rho(\text{crit})$, then $E_F > 1.3$ MeV. In such case protons capture electrons (inverse β -decay) to become neutrons, but the neutrons cannot decay back into protons and electrons. This is the phenomenon called neutronization.

We calculate the energy required for neutronization. Consider breaking a nucleus of ^{56}Fe up into 56 free neutrons. This is the inverse of the many nuclear reactions that fused 56 p or n into an iron nucleus. Then $\Delta mc^2 \approx 8 \times 10^{-4}$ ergs/Fe nucleus (from the binding energy of Fe). One Solar mass of pure ^{56}Fe has 2×10^{33} gm/ $[56 \times 1.6 \times 10^{-24}$ gm/Fe nucleus], so about 2×10^{55} Fe nuclei. The total energy required for neutronization is then 1.8×10^{52} ergs. We also must replace the energy carried off by the neutrinos during the 2 days of Si burning, which is about 10^{50} ergs.

The energy released during the collapse due to the difference in gravitational binding energy (6×10^{53} ergs) is more than sufficient to cover these two items.

The pressure at this ρ and T is largely from the degenerate free electrons. If as ρ increases, the free e^- are removed in producing the large number density of neutrons, the pressure may not increase much, if at all, and γ_{ad} will decrease. It can in this way decrease below $4/3$, the critical value for dynamical stability.

1.6. Neutrino Losses

There are substantial neutrino losses associated with the process of neutronization, 1 for every proton in a ^{56}Fe nucleus. There are roughly 10^{57} free electrons in a $1.4M_{\odot}$ Fe core, one for each proton in the Fe nuclei, which produce roughly 10^{57} ν_e . Each neutrino has an energy of roughly 10 MeV per electron captured, so (recall that $1 \text{ eV} = 1.6 \times 10^{-12} \text{ ergs}$) this leads to a total emitted energy in neutrinos of about 10^{52} ergs. The energy emitted via neutrinos of a SN is larger than that emitted in photons.

The predicted energy of the emerging neutrinos can be found by considering the core luminosity, $L_c = 4\pi R_c^2 \sigma T_c^4$. Recall that for a mean free path for ν in the core of l , the escape time is $t = R_c^2/(lc)$. $\rho > 3 \times 10^{11} \text{ gm/cm}^3$ is required for neutrino trapping. In that case, the density is high enough that the neutrinos cannot just stream out, in which case t would be R_c/c ; the actual escape time is a factor of R_c/l slower.

This then becomes similar to propagation of light through the star emerging from its atmosphere, and there is a corresponding neutrino atmosphere surface, which is located 1 mean free path length as calculated for neutrinos below the outer surface of the star, much deeper than the corresponding location of $\tau = 1$ for photons. We then have:

$$T_{eff}^4 = T_c^4 \frac{l}{R_c}$$

with l evaluated for neutrinos in the stellar core. Assuming $l \sim 10^{-4}R_c$ we find $10T_{eff}(\nu) = \langle T_c \rangle$.

We can use the observations of SN 1987A, where the typical observed ν had an energy of about 10 MeV to find that the mean T in the core corresponded to $KT \sim 100 \text{ MeV}$, which corresponds to $T \sim 10^{12} \text{ K}$.

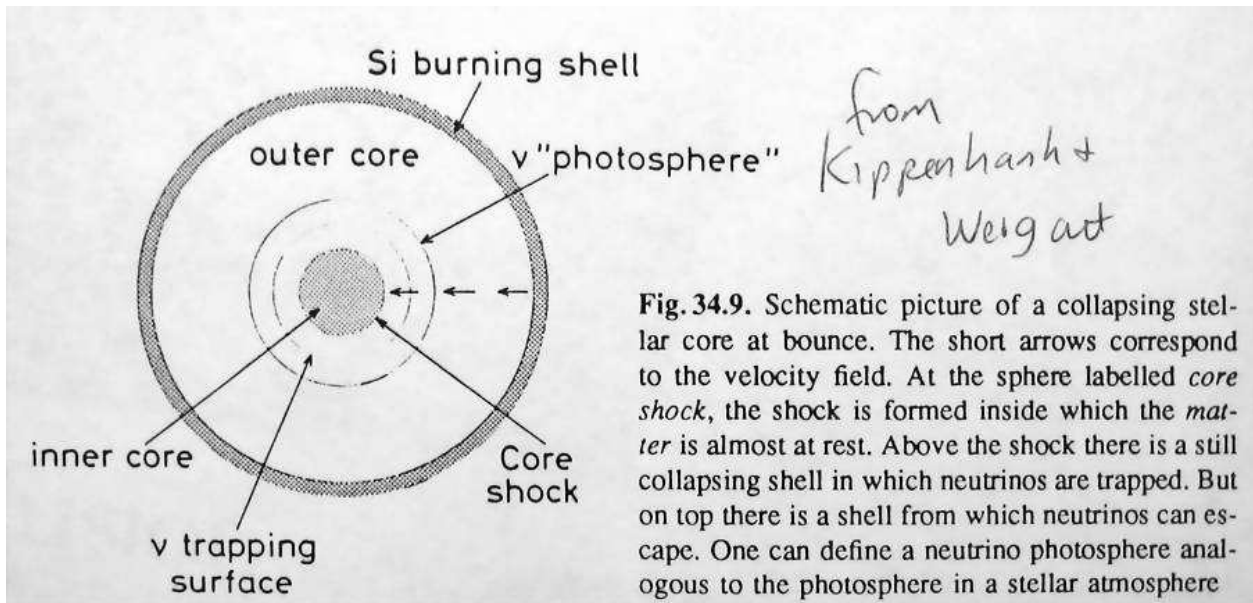


Fig. 2.— A schematic of the core of a massive star just prior to collapse. The surface from which the neutrinos come is indicated as the ν trapping surface. (Figure from KW)

1.7. Pair Creation

If a photon has energy $> 2m_e c^2$, then the usual pair annihilation, $e^- + e^+ \rightarrow 2\gamma$ can proceed in reverse, i.e. pair creation. Pair creation reduces γ_{ad} , effectively behaving like an ionization zone. This can fall below 4/3, which is the value required for dynamical instability. Once ρ becomes very high, pair creation is suppressed because the lower energy states for the electron are all filled.

1.8. Progenitor

In at least two cases (for SN1987A in the LMC and for SN1993J in the nearby galaxy M81) the progenitor star (the star before it exploded) was identified through archival images. In both cases, it appeared to be a luminous supergiant.

1.9. Ejected Material

The outer layers of a massive star undergoing core collapse do not collapse. We found above that the collapse time is less than 1 sec. The core radius prior to collapse is that of a white dwarf, $\sim 10^{-2}R_\odot$. But the total stellar radius is perhaps $10 R_\odot$ based on the scaling we found earlier, $R \propto M^{0.75}$. The timescale for the outer parts of the star to find out about the collapse is $\sim R/c_s$, where c_s is the speed of sound in the gas. But $c_s = \sqrt{\gamma P/\rho}$. For the outer parts of the star, $c_s \sim 10^7$ cm/sec. It will thus take $7 \times 10^{11}/10^7 = 7 \times 10^4$ sec for the outer parts of the star to be aware of the collapse of the stellar core. This is a factor of more than 10^5 times longer than the duration of the collapse, so even if our rough guess for c_s is off by 100, it does not matter.

So the core collapses very rapidly while the outer parts of the star hang suspended over it.

Much of the material in the outer parts of the star may subsequently fall onto the core, while much material may be ejected by the explosion that follows. The exact mechanism of the explosion/ejection of material (shocks presumably) is not well understood.

The SN produces large amounts of Fe-peak elements Co, Fe and Ni, some of which end up being ejected. The initial ^{56}Ni decays with a 6.1 day half life into ^{56}Co , which decays with a 77 day half life into ^{56}Fe , a stable nucleus. After the shocks of the initial SN explosion (which determine the early time light curve) have faded away, these radioactive decays power the SN, and we can predict the late time luminosity of the SN directly from their energy input, as is shown in the figures. Furthermore we can directly detect strong emission lines of Fe, Ni and Co in the optical, IR and γ -ray spectra of SN to establish the presence of a substantial amount of Fe-peak nuclei.

Once the SN fades below detectability, we should see the remnant (a pulsar or a neutron star). The search for the remnant of SN 1987A has not yet yielded a detection of such, which is somewhat surprising. But neutron star remnants have been detected for some Galactic SN, some of which are seen as pulsars, with a few detected in deep images as point sources. (See the paper “Limits on the Detection From the HST on a Point Source in SN 1987A” by Graves et al, 2006, which also includes a table of the Galactic remnant detections.)

The expansion of the remnant can be measured through comparison of a set of images taken over several years – this yields the velocity of the debris, not of the initial SN, which is determined from the width of spectral features near maximum light. The former is about 3000 km/sec for SN 1987A, while the latter is closer to 25,000 km/sec in most cases.

The ejected material will contain lots of light elements such as C, N, O, Mg, etc from the onion skin outer layers of the star, which represent the ashes from previous epochs of nuclear burning, and which are ejected in their entirety, as well as some Co, Fe and Ni from

the region closer to the core. This ejected material will mix with the ISM (which may also contain much material previously lost from the star). This forms the supernova remnant, a large complex region around the SN which can be studied in detail with spectroscopy at various wavelengths. The ejected material will enhance the heavy element content of the ISM and thus of the next generation of stars that form from this gas. The details of this depend on the mass cut for fallback, the initial mass of the star and the mass lost prior to core collapse. as well as on the energy of the SN.

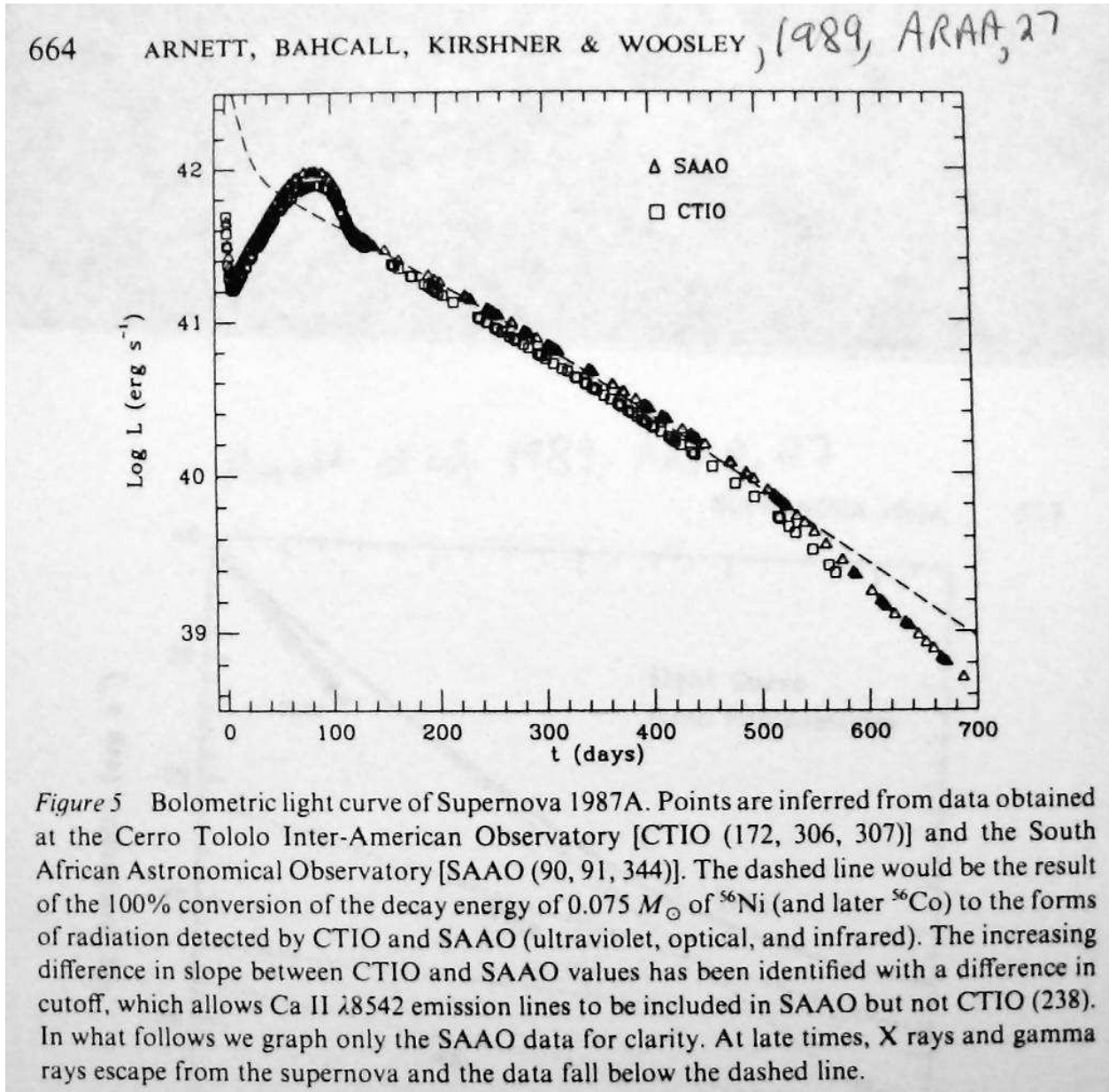


Fig. 3.— The bolometric light curve for SN 1987A up to 700 days after the explosion. The dashed line is that predicted based on radioactive decays of $0.08 M_{\odot}$ of ^{56}Ni decaying to ^{56}Co and then to ^{56}Fe . (Figure from review by Arnett et al, 1989, ARAA, 27)

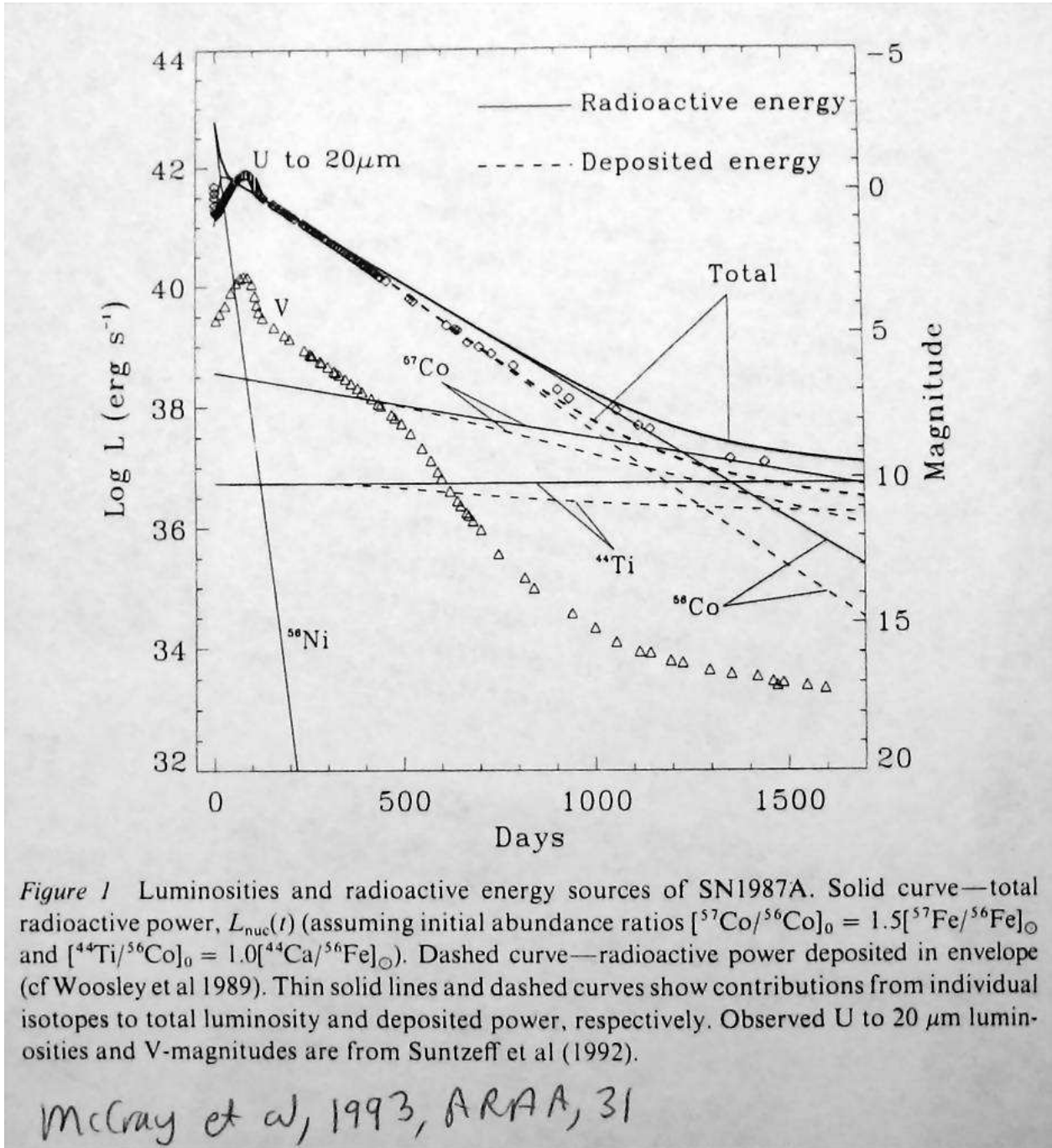


Fig. 4.— The predicted luminosity of SN 1987A at late times compared to that predicted from radioactive decays. (Figure from review by McCray et al, 1989, ARAA, 31)

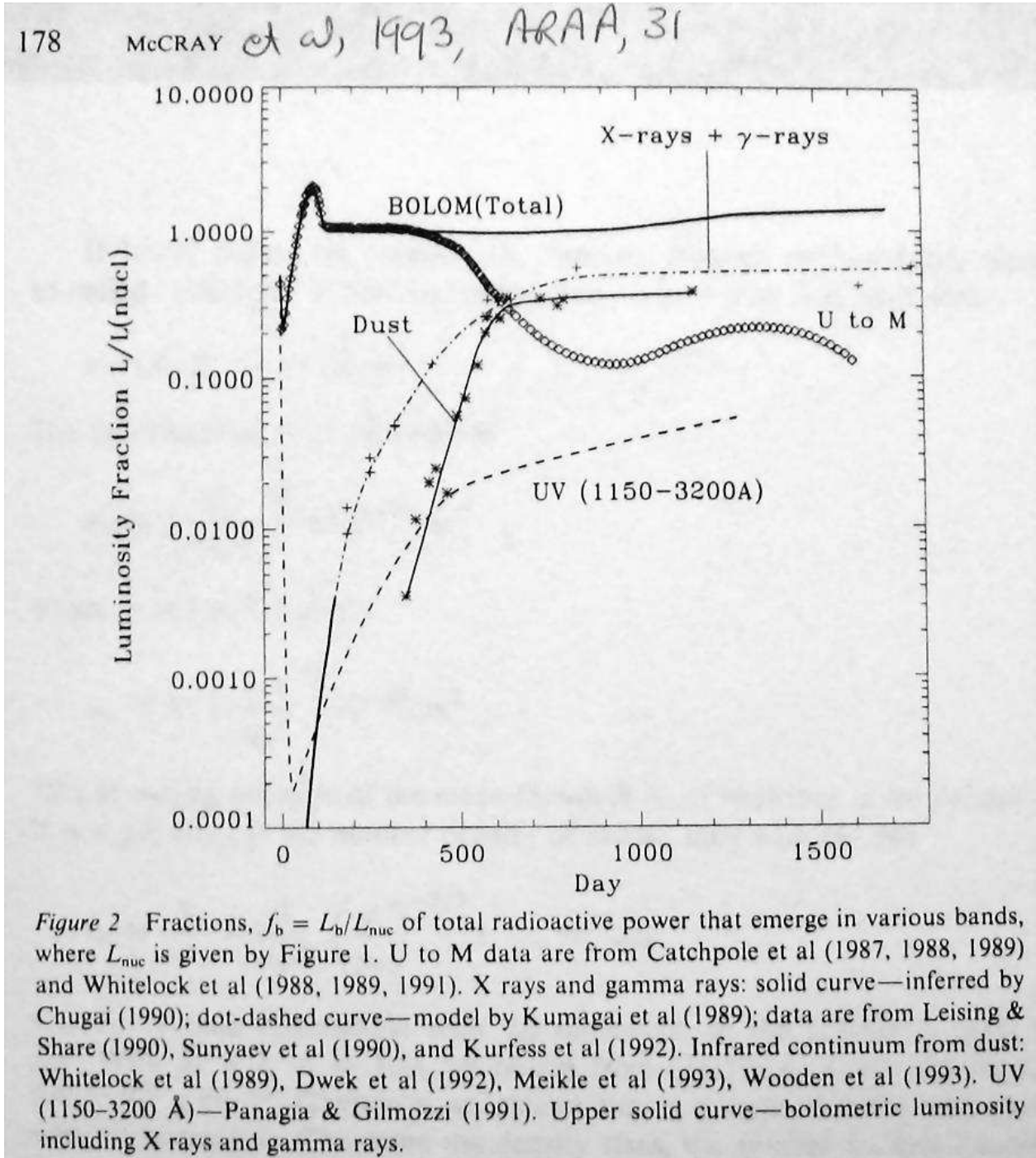


Fig. 5.— The predicted luminosity of SN 1987A with the contributions over various wavelength regimes indicated. Note the importance of dust at late times. (Figure from review by McCray et al, 1989, ARAA, 31)

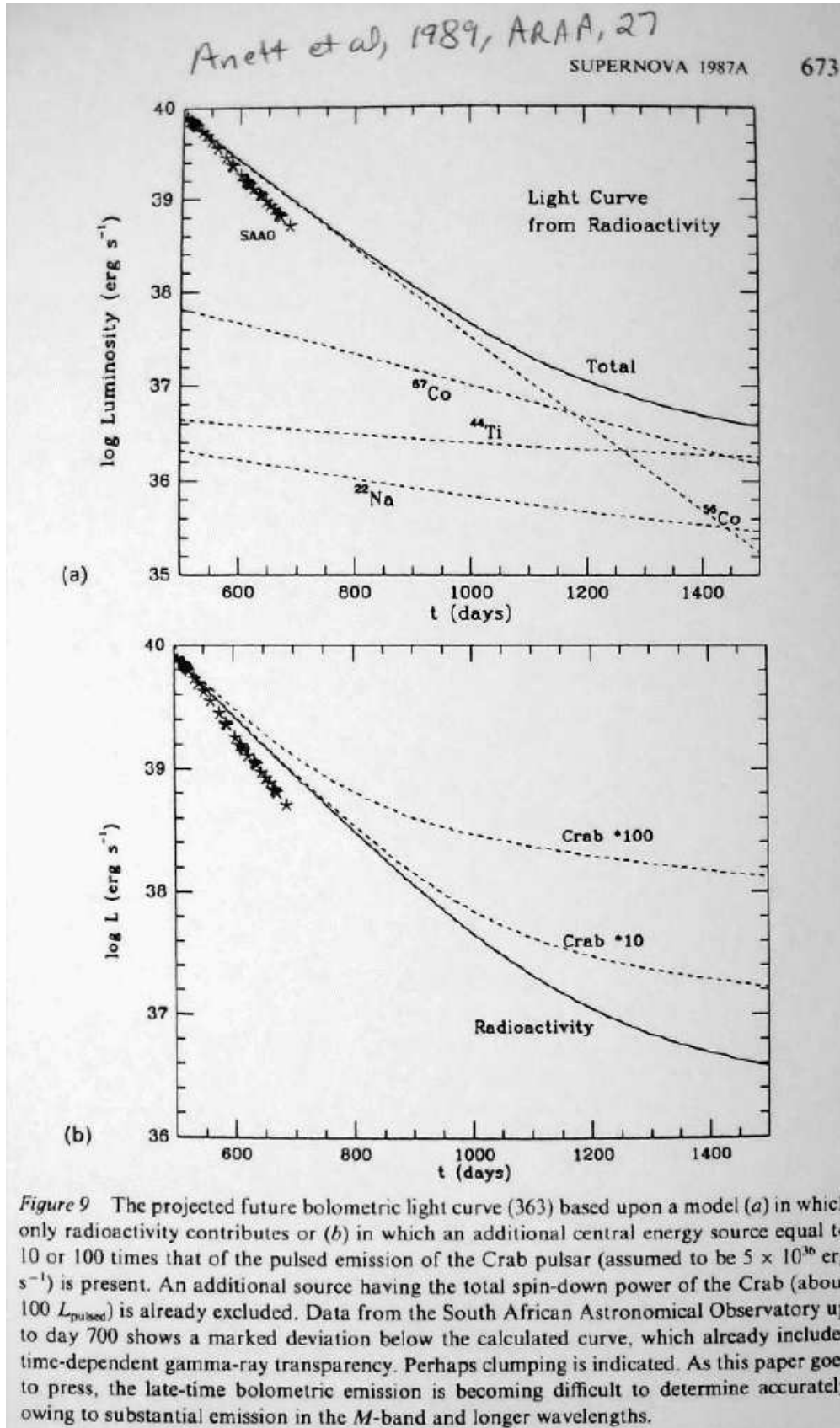


Fig. 6.— The search for a remnant in SN 1987A. Predicted light curves for radioactive

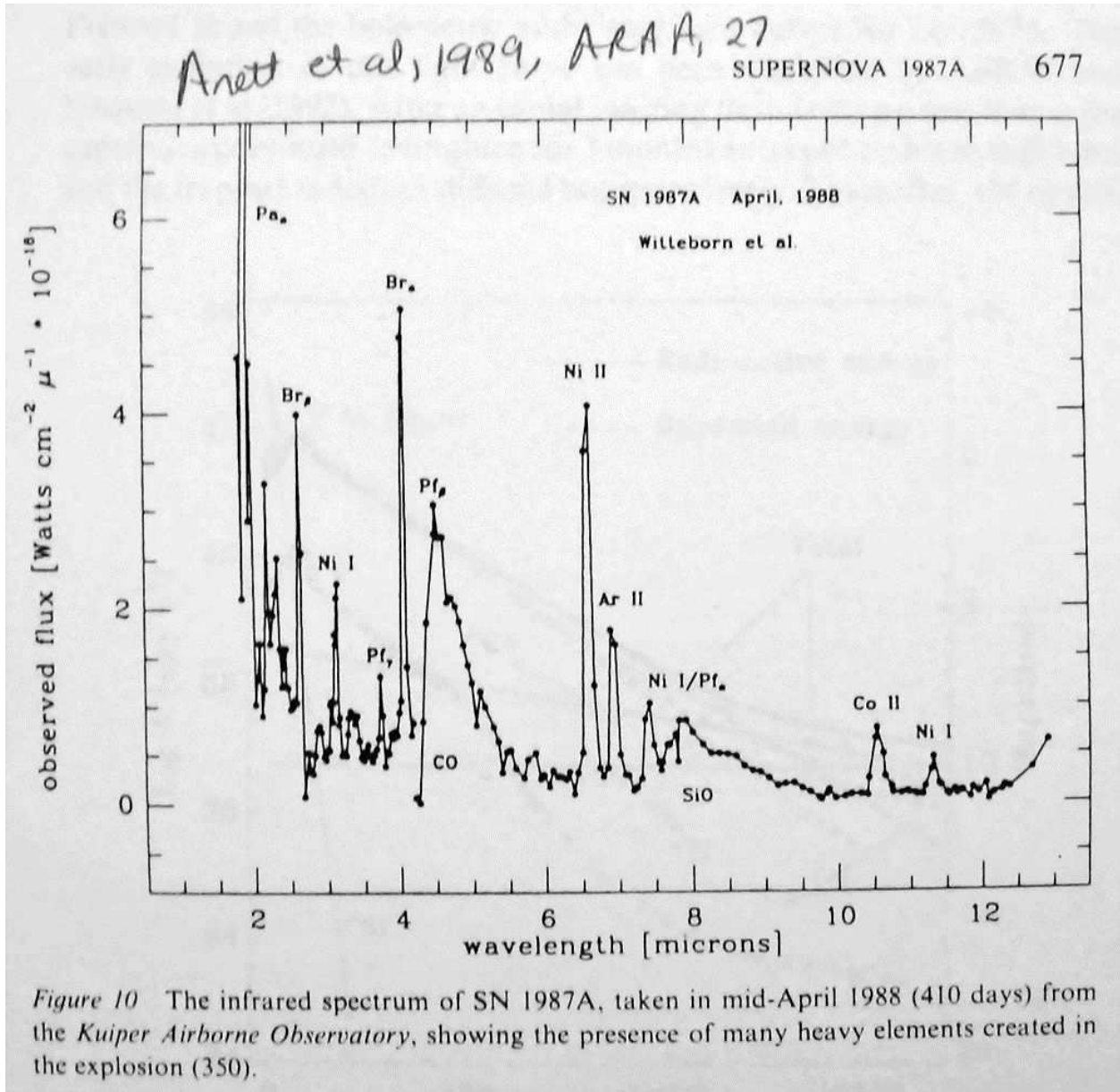


Fig. 7.— The infrared spectrum of SN 1987A take 410 days after the explosion. Note the presence of unepctedly strong lines of Ni and of Co, which normally are not detectable. (Figure from review by Arnett et al, 1989, ARAA, 27)

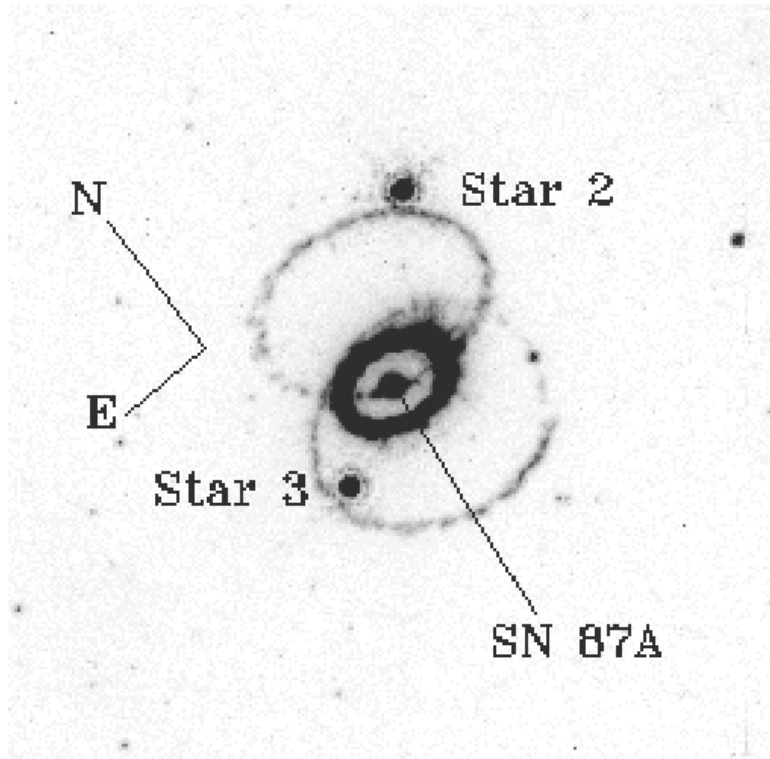


Figure: WFPC2 image of SN 1987A and its neighborhood, taken with the F814W (I) filter on 1994 September 24 (day 2770)

Fig. 8.— The debris from the explosion of SN 1987A viewed at late time (day 2770), as seen by WFPC2 on HST with a F814W filter (see www.stsci.edu/stsci/meetings/shst2/puncs.html). The expansion velocity of the debris measured with a time sequence of images is ~ 3000 km/sec. The rings represent material ejected from the aging star prior to the SN that were ionized by the UV photons from the SN event – they are not part of the actual SN ejecta, which at the time this image was obtained, was still very small in apparent diameter. Note that the previous ejection episodes must have been highly aspherical.

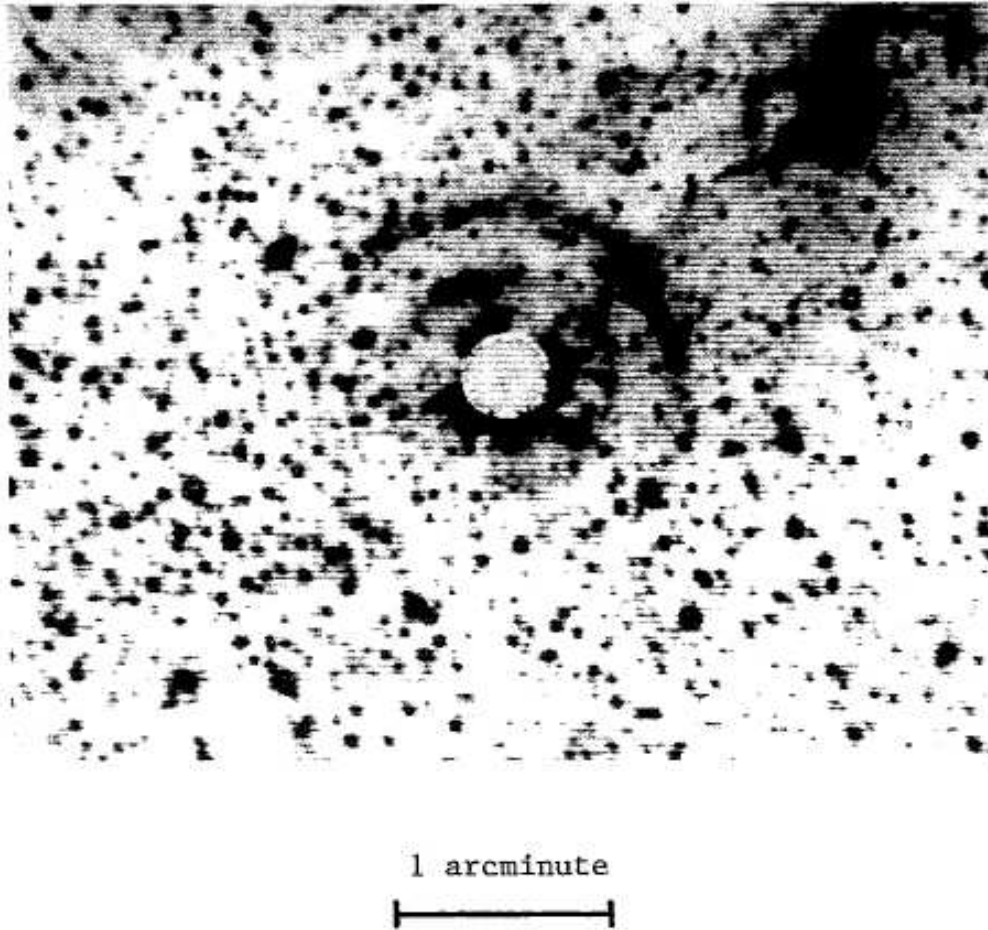


Fig. 9.— The light echo of SN1987A as seen in 1988, from Crotts, 1988, ApJL, 333, L51.
This allows study of the ISM and previously ejected material around the SN.

2. Type Ia Supernovae

SNIa are very different from SNII. Their spectra show no signs of hydrogen. Their spectra and light curves are more homogenous, and they are more luminous, than are SNII. It is for these reasons that SNIa have become important tools for cosmology, behaving as standard candles that can be identified and monitored for 100 days or more on the ground out to redshifts near 1 and to even larger redshifts from HST.

The lack of H in their spectra means that the progenitor star of a SNIa must have lost its entire outer envelope down to the radius at which H has been converted into He. This is only possible at late stages of stellar evolution.

No neutron star remnant has been detected for any SNIa.

Their suggested origin is a thermonuclear explosion on a C+O white dwarf near the Chandrasekhar mass, which somehow receives additional material to reach a mass higher than that limit. The ignition of fuel in a degenerate white dwarf could produce an detonation similar to a bomb. The white dwarf origin imposes a very limited mass range for SNIa progenitors, and helps ensure the observed uniformity of their properties. Since the progenitor star is suspected to be a white dwarf, i.e. of very low luminosity, it is no surprise that no progenitor star has been identified for any SNIa in a nearby galaxy.

There have been two suggested mechanisms to achieve SNIa. The first involves accretion from some companion object, while the second involves the merging of two white dwarfs in a close binary system. This merging is sure to happen due to loss of energy via gravitational radiation. At present, given the continued uniformity observed for SNIa events even as the samples of well studied objects grow larger, the accretion model onto a single white dwarf seems to be favored.

The late time light curves show the characteristic declining exponential one expects

from input of energy from radioactive decays discussed earlier for SNII. SNIa light curves and spectra can be modelled fairly well.

The spectra of SNIa show the presence of some light elements (Ca, Si) as well as the Fe-peak elements. Thus the early models assuming a detonation wave sweeping over the entire star at the speed of sound have been ruled out, as in this case all the stellar matter would have been converted to Fe-peak elements.

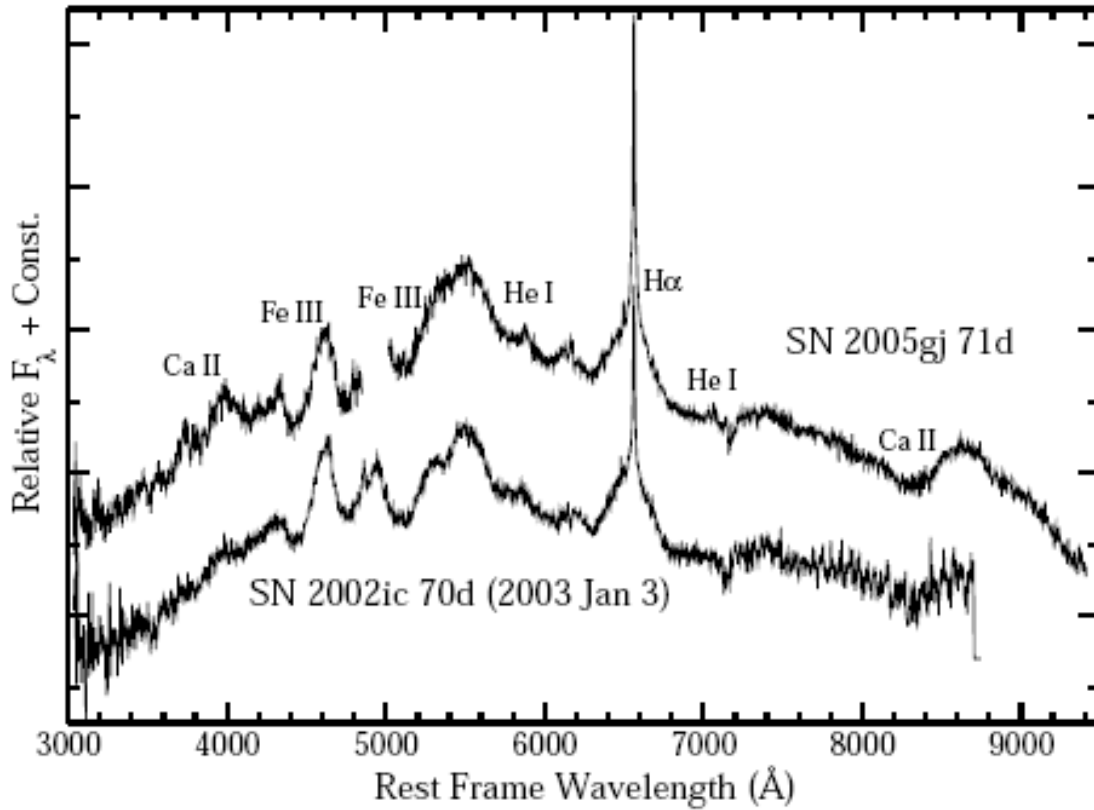


Fig. 6.— Comparison of the spectrum of SN 2005gj 71 days after explosion with that of SN 2002ic at approximately the same phase (assuming an explosion date of 2005 November 5 UTC for SN 2002ic).

Fig. 10.— The spectra of two local SNIa. Note the absence of hydrogen and the very broad lines of Ca and Fe. The narrow H α line is coming from circumstellar or interstellar material around the SN, not from the SN itself. (from Aldering et al, 2006, ApJ)

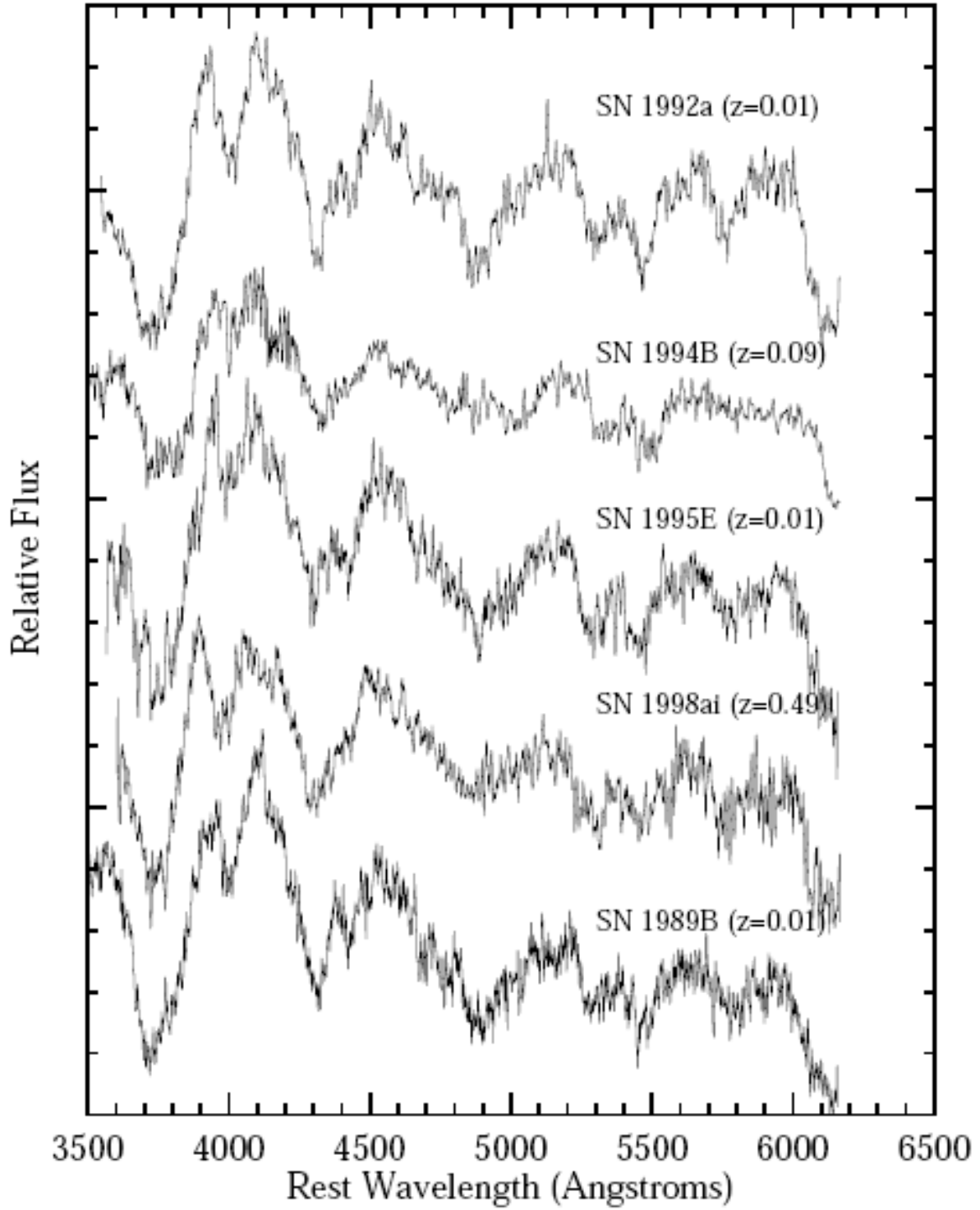
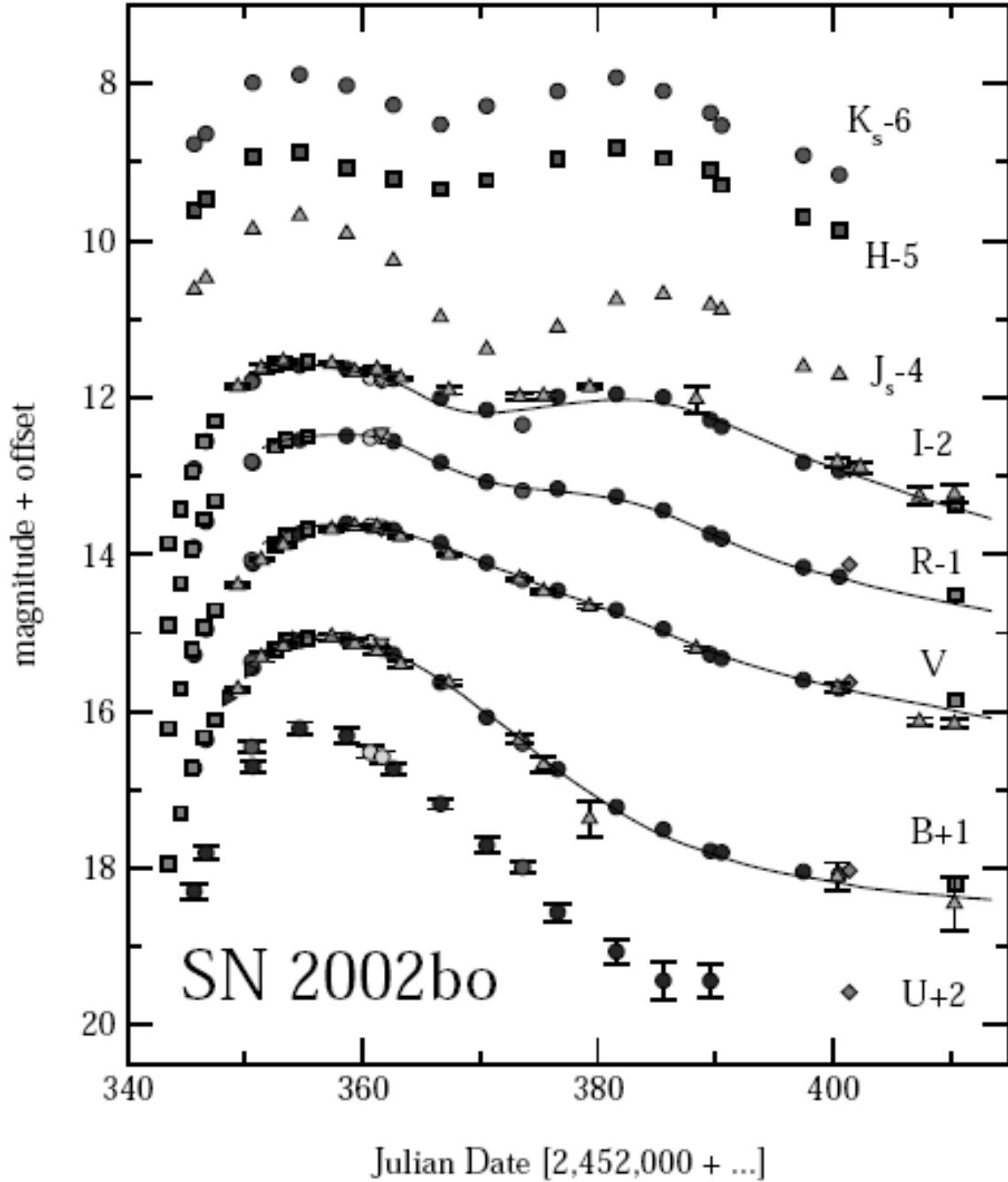


Fig. 11.— Optical spectra of a collection of local and intermediate redshift SNIa are compared, shifted to the rest frame of each.



Krisciunas *et al.* Fig. 9

Fig. 12.— Multi-color light curves for the nearby SN 2002bo from the UV to the IR. Figure from Krisciunas, Suntzeff, et al, 2005, ApJ.

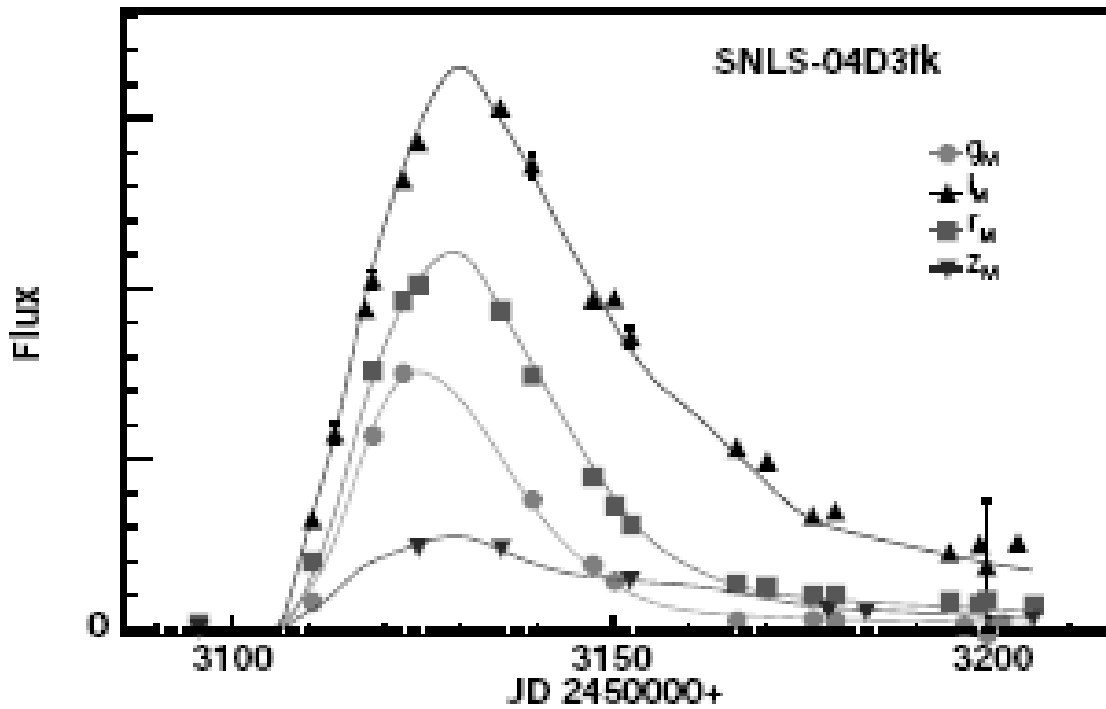
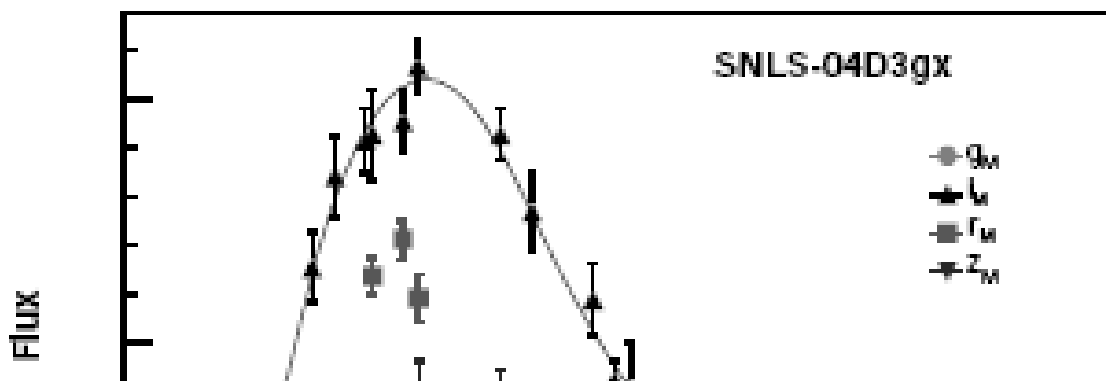


Fig. 1 Observed light-curves points of the SN Ia SNLS-04D3fk in g_M , r_M , i_M and z_M bands, along with the multi-color light-curve model (described in Section 5.1). Note the regular sampling of the observations both before and after maximum light. With a SN redshift of 0.358, the four measured pass-bands lie in the wavelength range of the light-curve model, defined by rest-frame U to R bands, and all light-curves points are therefore fitted simultaneously with only four free parameters (photometric normalization, date of maximum, a stretch and a color parameter).



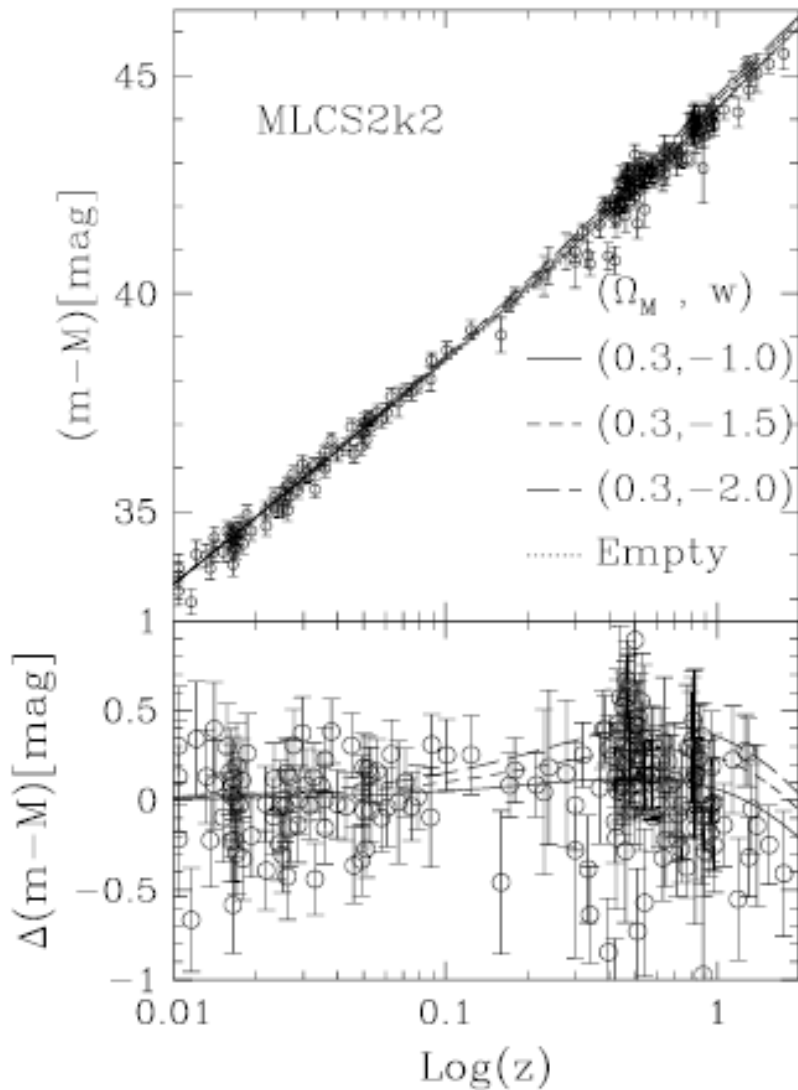


Fig. 22.— The Hubble diagram including the SNe presented in this study, using solid symbols, and those of Riess et al. (1998) and Tonry et al. (2003), using open symbols. Error bars correspond to 1σ . The upper panel shows the standard diagram, including the curves corresponding to the luminosity distances for universes with various parameters, as given in the legend. The lower panel shows the differential Hubble diagram, where the ordinate corresponds to the difference between the distance moduli observed (for SNe) and computed (for models) with the empty universe. The legend for line types is the same as in the upper panel.

Fig. 14.— The Hubble diagram for SNIa showing how they are used as standard candles for cosmology. This Fig. is from “HST and Ground Based Observations of SNIa...” Clocchiatti, Schmidt, Filippenko..., 2006.

3. SN Searches

In the 1940s, Fritz Zwicky searched for SN using the Palomar Schmidt, which he had built specifically for this purpose. Now, with the importance of SNIa for cosmology, an enormous effort is going into finding and characterizing SN, with the required spectroscopic follow up concentrating mostly on SNIa.

Among the ongoing surveys are:

(Local Surveys) Nearby SN Factory (detection and spectroscopic followup, uses digital image survey at Palomar Schmidt), Carnegie SN project (IR light curves and optical spectroscopy), SDSS SN Survey - just starting up

(Distant SN):

Supernova Legacy Survey (CFHT) in their first year's operation of a planned 5 years they found 71 high redshift SN Ia with the Megacam at the CFHT using repeated imaging of four 1 sq deg fields in 4 bands. Extensive followup with Keck and VLT for spectroscopy.

ESSENCE: a 5 year ground based project to detect 200 SN Ia $0.2 < z < 0.8$

Many other such surveys, both ground based and space based (proposed Dark Energy Mission) are in the planning or early implementation phases.